A Study of Optical Sensor Based on Fiber Bragg Grating (FBG) Using COMSOL Multiphysics

C. Gavrila[*1], I. Lancranjan[2]
[1] Technical University of Civil Engineering Bucharest, Romania,
[2] Advanced Study Centre - National Institute for Aerospace Research "Elie Carafoli", Bucharest, Romania
*Corresponding author: 66, Pache Protopopescu Blvd, Sector 2, 021414 Bucharest, Romania, cgavrila2003@yahoo.com

Abstract: Fiber optic sensors can measure a large range of physical, chemical and environmental variables such as temperature, pressure, shape, position, chemical concentration, moisture, etc. Fiber optic sensors provide measurements in applications where the conventional electrical based sensors cannot be used, due to measurement requirements such as extreme temperature, small size, high sensor count, or high electromagnetic energy or radiation environments. In this paper, we propose a study of an optical sensor based on a Fiber Bragg Grating (FBG) setup arrangement using COMSOL Multiphysics. The effect of environmental parameters on the composite material machine part is observed by the modification of the length (L) of the Fabry-Perot interferometer formed by two Bragg grating mirrors. This variation can be studied by a transmission spectroscopy measurement. The developed COMSOL Multiphysics sensor model takes into account the interaction of Fiber Bragg Grating (FBG) with composite material.

Keywords: Fabry-Perot Interferometer, optic fiber, Bragg grating reflector

1. Introduction

The paper presents an attempt in modeling a new class of sensors used into an increasing number of applications, namely the Bragg grating fiber optic sensors. In-fiber grating-based sensors have many advantages over conventional electric and alternative fiber optic sensor configurations. They are relatively straight-forward, inexpensive to produce, immune to electromagnetic (EM) interference and interruption, lightweight, small in size, and self-referencing with a linear response. Most significantly, their wave-length-encoding multiplexing capability allows tens of gratings in a single piece of fiber to form an optical data-bus network. The combination of their multiplexing capability and inherent compatibility with fiber reinforced composite materials permits in-fiber gratings to be embedded in a number of important structural materials for smart structure applications [1 – 7].

2. Theory

In Figure 1, the schematics of a fiber optic sensor using a Fabry-Perot interferometer (FPI) is presented. It is formed by two Bragg grating reflectors of reflectance R_1 and R_2 separated by a fiber optic portion of length L.

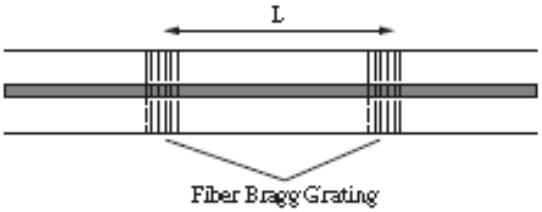

Figure 1 - Schematic of the analyzed Fiber Bragg Grating sensor.

The individual Bragg grating reflectors in the FPI can be characterized by transmittances T_i and reflectance R_i, i = 1, 2, such that $R_i + T_i = 1$ The Fabry–Perot reflectance R_{FP} and transmittance T_{FP} are found to be

$$R_{FP} = \frac{R_1 + R_2 + 2\sqrt{R_1 R_2}\cos\phi}{1 + R_1 R_2 + 2\sqrt{R_1 R_2}\cos\phi} \quad (1)$$

$$T_{FP} = \frac{T_1 T_2}{1 + R_1 R_2 + 2\sqrt{R_1 R_2}\cos\phi} \quad (2)$$

R_{FP} represents the ratio of the power reflected by the FPI, P_r, to the incident power on the FPI, P_i. T_{FP} is the ratio of the transmitted power P_t to the incident power, P_i. represents the round-trip propagation phase shift in the interferometer, defined by:

$$\phi = \frac{4\pi n L}{\lambda} \quad (3)$$

In Eq. (3) n is the refractive index of the region between the mirrors and λ the free space optical wavelength. It has been assumed that the light experiences a $\pi/2$ phase shift at each reflection, as appropriate for dielectric mirrors, which is added to the propagation phase shift of Eq. (3).

It is evident from Eq. (2.2) that T_{FP} is a maximum for

$$\cos\phi = -1 \quad (4)$$

and

$$\phi = (2m+1)\pi \quad (5)$$

with *m* an integer. If we define

$$\Delta = \phi - (2m+1)\pi \quad (6)$$

then near a maximum in T_{FP},

$$\cos\phi \approx -\left(1 - \frac{\Delta^2}{2}\right) \quad (7)$$

with

$$\Delta \leq 1 \quad (8)$$

In the case that the mirror reflectances are equal and approach unity, then Eq. (2) simplifies to

$$T_{FP} = \frac{T^2}{(1-R)^2 + R\Delta^2} \quad (9)$$

where $R = R_1 = R_2$ and $T = 1 - R$. The maximum transmittance occurs when $\Delta = 0$ [1-5].

Another limiting case where the mirror reflectances are low is of particular interest in the case of the fiber Fabry–Perot sensors. Assuming once again that the mirrors have equal reflectances, it follows from Eqs. (1) and (2) that if $R << 1$, then

$$R_{FP} = 2R(\cos\phi + 1) \quad (10)$$

and

$$T_{FP} \cong 1 - 2R(\cos\phi + 1) \quad (11)$$

The fiber Fabry–Perot sensors that have evolved from early works are generally classified as intrinsic or extrinsic. In both intrinsic and extrinsic sensors, a fiber (in most cases, single mode) transports light from an emitter to the interferometer and from the interferometer to a photo detector. In an intrinsic fiber Fabry–Perot interferometer sensor, generally termed an "FFPI" sensor, the two mirrors are separated by a length of single-mode fiber and the measured affects the optical path length of the light propagating in the fiber itself. In an extrinsic fiber-based Fabry–Perot sensor, generally referred to as an "EFPI" sensor, the two mirrors are separated by an air gap or by some solid material other than the fiber. Thus, in the EFPI sensor the measured affects the optical path length in a medium other than the fiber that transports the monitoring light to and from the interferometer. Both FFPIs and EFPIs are designed such that a measured affects the optical length of the cavity, and light reflected or transmitted by the interferometer is converted by a photo detector to an electrical signal that is processed electronically to evaluate the measured.

The analysis of the schematic of a Fiber Bragg Grating sensor presented in Figure 1 leads to an elementary study of Bragg grating reflector. It consists of a short section of single-mode optical fiber in which the core refractive index is modulated periodically. As depicted in Figure 2, this structure acts as a highly wavelength-selective reflection filter with the wavelength of the peak reflectivity, λ_B, determined by the phase matching condition.

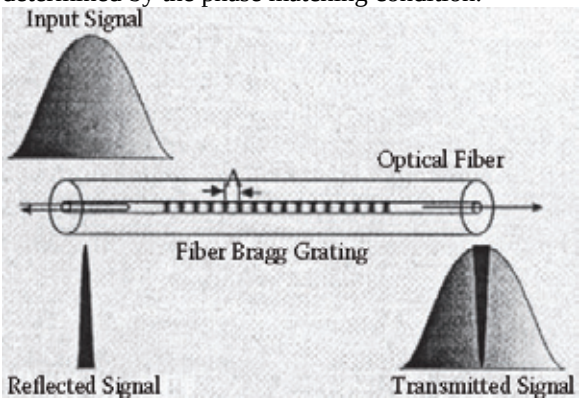

Figure 2 - Schematic diagram of structure and spectral response of fiber Bragg grating.

The wavelength of the peak reflectivity, λ_B, is defined as

$$\lambda_B = 2n_{eff}\Lambda \quad (12)$$

where n_{eff} is the effective refractive index of the guided mode in the fiber, and Λ is the period of the refractive index modulation with a form of

$$n(z) = n_{co} + \delta n\left(\cos\left(\frac{2\pi z}{\Lambda}\right) + 1\right) \quad (13)$$

In Eq.(13) n_{co} is the unexposed core refractive index and δn is the amplitude of the photo-induced index excursion. This periodical index-modulated structure enables the light to be coupled from the forward-propagating core mode into the backward-propagating core mode, generating a reflection response [1 – 7].

The sensing function of an FBG derives from the sensitivity of both the refractive index and grating period to externally apply mechanical or thermal perturbations. The strain field affects the response of an FBG directly, through the expansion and compression of the grating pitch size and through the strain-optic effect—that is, the strain-induced modification of the refractive index. The temperature sensitivity of an FBG occurs principally through the effect on the induced refractive index change and, to a lesser extent, on the thermal expansion coefficient of the fiber. Thus, the peak reflected wavelength shifts by an amount $\Delta\lambda B$ in response to strain ε and temperature change ΔT as given by

$$\frac{\Delta\lambda_B}{\lambda_B} = P_e\varepsilon + \left[P_e\left(\alpha_s - \alpha_f\right) + \xi\right]\Delta T \quad (14)$$

The sensor function of the setup presented in Figure 1, a setup based on the use of a Fabry – Perot etalon formed of two Bragg grating reflectors, is

performed by temperature and strain induced variations of L and/or λ_B [4 – 11].

3. Results and Discussion

The COMSOL Multiphysics program is used to simulate the propagation of the test laser beam inside a mono mode fiber optic in order to evaluate the Fabry-Perot interferometer transmittance. The variations of the two Bragg reflectors composing the Fabry-Perot interferometer are considered. According to the COMSOL Multiphysics simulation results, the role of Bragg grating reflectivity variation is dominant into the total Fabry-Perot etalon transmittance. We select **3D** as the **Space Dimension**, then in the list of **Physical Models** the following menu link is selected: **COMSOL Multiphysics > PDE Modes > Classical PDEs > PDE, General Form**. We build the geometry of the Fabry-Perot interferometer composed of two Bragg grating reflectors embedded into a piece of composite material of a common structure for aeronautical applications. In the next step we fix the boundary settings, the mesh parameters (Figures 3, 4 and 5) and compute the final solution, namely the variation of Fabry-Perot etalon transmittance with its length, for various values of Bragg grating reflectivity (Figure 6).

Figure 3 - Geometry of the Bragg grating fiber optic embedded composite material.

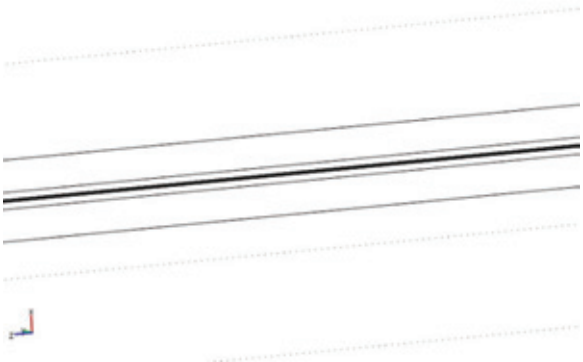

Figure 4 - Details of the geometry of the Bragg grating fiber optic embedded composite material. The core and cladding of Bragg grating fiber optic can be observed.

Figure 5 - Geometry of the Bragg grating fiber optic embedded composite material. The COMSOL mesh grid can be observed.

In order to obtain more realistic results of the COMSOL Multiphysics simulation of the Fabry-Perot interferometer with Bragg reflectors embedded into a composite material, several usual receipts of it were considered. In Table 1 the materials used as the ingredients of these receipts are presented. The basic rule of thumb of these receipts was that the external layers of the analyzed composite materials are made of glass fiber, Kevlar or carbon fiber. In Table 1 the considered thickness of each layer is mentioned.

Table 1: The materials used for designing the composite material test piece containing the embedded Bragg grating fiber optic.

Material	Thickness
COREMAT Lantor	3 ÷ 5 mm
Glass fiber sheet	250 ÷ 500 μm
Carbon fiber sheet	250 ÷ 500 μm
Kevlar sheet	250 ÷ 500 μm
Epoxy Resin	250 ÷ 500 μm

The parameters of Bragg grating optic fiber were taken from common data sheets, especially the geometric ones. This means that for building the COMSOL Multiphysics model geometry the total optic fiber diameter was considered to be of 250 μm. The core of the analyzed fiber optic sensor was considered of 75 μm. The very different values of the geometric parameters created some difficulties in building the COMSOL Multiphysics model geometry. The strain and/or temperature mechanical loads of the composite material test pieces were considered to modify the length L of the Fabry – Perot etalon, and implicitly its transmittance. The variation of the two Bragg grating reflectivity was modeled by considering the temperature and/or strain induced variation of the effective refractive index of the guided mode in the fiber, n_{eff} and of the period of the refractive index modulation, Λ.

In Figure 6 the simulation results obtained in the case of Fabry-Perot etalon transmittance variation with L for several values of Bragg grating reflectivity

R_1 and R_2 are presented. The Bragg grating reflectivity R_1 and R_2 were considered into two value domains, namely very high (>0.90- black curve) and very low (< 0.4 – red curve).

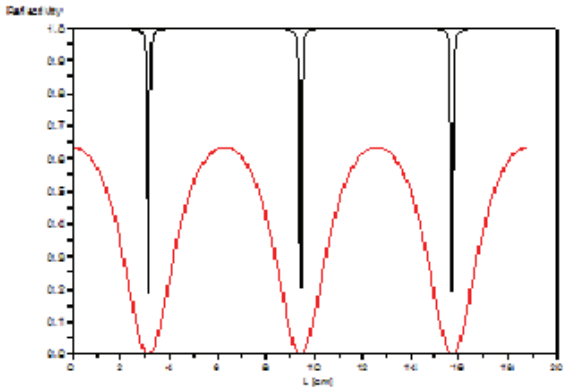

Figure 6 – The simulation results obtained for the variation of Fabry-Perot etalon transmittance with its length.

Black curve - $R_1=0.90$ and $R_2=0.95$
Red curve - $R_1=0.45$ and $R_2=0.38$.

4. Conclusions

In this paper we have demonstrated the versatility of COMSOL Multiphysics regarding the modeling and simulation of fiber optic sensor based on the use of the Fabry - Perot etalon composed of Bragg grating reflectors.

The obtained COMSOL Multiphysics models are under development for fulfillment of aeronautic industry design needs. The considered development includes comparison with experimental results.

5. References

1. I. Bennion, J. A. R. Williams, L. Zhang, K. Sugden, and N. J. Doran, UV-written in-fiber Bragg gratings, *Opt. Quantum Electron.*, **28**, pp. 93–135, 1996.
2. R. Kashyap, *Fiber Bragg Gratings*, Academic Press, New York, 1999.
3. A. Othonos and K. Kalli, *Fibre Bragg Gratings: Fundamentals and Applications in Telecommunications and Sensing*, Artech House, London, 1999.
4. K. O. Hill and G. Meltz, Fiber Bragg grating technology fundamentals and overview, *J. Lightwave Tech.*, **15**, pp. 1263–1276, 1997.
5. Y. J. Rao, In-fiber Bragg grating sensors, *Measurement Sci. Tech.*, **8**, pp. 355–375, 1997.
7. S. Kannan, J. Z. Y. Guo, and P. J. Lemaire, Thermal stability analysis of UVinduced fiber Bragg gratings, *J. Lightwave Tech.*, **15**, pp. 1478–1483, 1997.
8. S. M. Melle, K. Liu, and M. Measures, A passive wavelength demodulation system for guided-wave Bragg grating sensors, *IEEE Photon. Technol. Lett.*, **4**, 5, pp. 516–518, 1992.
9. M. A. Davis and A. D. Kersey, All-fiber Bragg grating strain-sensor demodulation technique using a wavelength division coupler, *Electron. Lett.*, **30**, pp. 75–77, 1994.
10. Q. Zhang, D. A. Brown, H. Kung, J. E. Townsend, M. Chen, L. J. Reinhart, and T. F. Morse, Use of highly overcoupled couplers to detect shifts in Bragg wavelength, *Electron. Lett.*, **31**, 6, pp. 480–482, 1995.
11. A. B. Lobo Ribeiro, L. A. Ferreira, M. Tsvetkov, and J. L. Santos, All fiber interrogation technique for fiber Bragg sensors using a biconical fiber filter, *Electron.Lett.*, **32**, 4, pp. 382–383, 1996.